ISSN: 2584-0355
DOI: doi.org/10.51219/MCCRJ/Eber-Luis-Steolo/525

URF PUBLISHERS
connect with research world

Medical & Clinical Case Reports Journal

https://urfpublishers.com/journal/case-reports

Vol: 4 & Iss: 3

Case Report

The First Dynamic Xilloc System for Total Temporomandibular Joint Replacement Performed in Germany: Technical Profile and Pioneer of a 6-year Follow-up Case Report of a Patient-Specific 3D-Printed Titanium Reconstruction

Short Title: Six-year Follow-up of the First Germany TMJ Total Joint Reconstruction using Xilloc System

Dr. Eber Luis Steolo[1]* and Prof. Dr. Peter Maurer[2]

[1]Oral and Maxillofacial Surgeon in the USA, Germany and Brazil; Active member of the American Society of TMJ Surgeon; Independent International Consultant for OMFS; Former Assistant Professor in the Oral and Maxillofacial Department at West Virginia University School of Dentistry, Morgantown - WV, USA; Independent Oral and Maxillofacial Surgeon at Praxisklinik Prof. Dr. Peter Maurer in Trier (Porta Nigra), Rhineland-Palatinate, Germany

[2]Oral and Maxillofacial Surgeon with Private Practice in Trier (Porta Nigra), Rhineland-Palatinte, Germany

Citation: Steolo EL, Maurer P. The First Dynamic Xilloc System for Total Temporomandibular Joint Replacement Performed in Germany: Technical Profile and Pioneer of a 6-year Follow-up Case Report of a Patient-Specific 3D-Printed Titanium Reconstruction. *Medi Clin Case Rep J* 2026;4(3):1982-1995. DOI: doi.org/10.51219/MCCRJ/Eber-Luis-Steolo/525

Received: 22 August, 2026; **Accepted:** 28 August, 2026; **Published:** 31 August, 2026

***Corresponding author:** Dr. Eber Luis Steolo, Oral and Maxillofacial Surgeon in the USA, Germany and Brazil; Active member of the American Society of TMJ Surgeon; Independent International Consultant for OMFS; Former Assistant Professor in the Oral and Maxillofacial Department at West Virginia University School of Dentistry, Morgantown - WV, USA; Independent Oral and Maxillofacial Surgeon at Praxisklinik Prof. Dr. Peter Maurer in Trier (Porta Nigra), Rhineland-Palatinate, Germany, ZIPCODE 85501-054, Brazil

Copyright: © 2026 Steolo EL, et al., This is an open-access article distributed under the terms of the Creative Commons Attribution License, which permits unrestricted use, distribution, and reproduction in any medium, provided the original author and source are credited.

ABSTRACT

Background: Managing end-stage Temporomandibular Joint pathologies presents a critical surgical and clinical hurdles in Oral and Maxillofacial Reconstructive Surgery. Conventional interventions, namely autogenous bone grafts and prefabricated stock prostheses, frequently prove inadequate when addressing profound anatomical deformities or satisfying the complex biomechanical requisites of the joint. To overcome these limitations, custom-engineered Temporomandibular Joint and patient-specific implants have emerged as a superior alternative, proven by the scientific literature in this field, providing precise adaptation to distorted osseous architecture, enhancing long-term implant survivability and restoring optimal Oral and Maxillofacial aesthetics.

Objective: To evaluate the long-term clinical viability of advanced additive manufacturing in Oral and Maxillofacial reconstruction, this paper outlines the surgical, technical and biomechanical specifications of the custom-made, Three-dimmensional printed Xilloc Temporomandibular Joint Prosthesis System for Total Joint Reconstruction. We report the 6-year longitudinal outcomes of the pioneering, first-in-country case report of a patient-specific Total Temporomandibular Joint Reconstruction performed in Germany, validating its durability and functional performance.

Case report: A 56 y.o. A.F. with severe bilateral TMJ osteoarthrosis, secondary to autoimmune disease, with an Maximum Mouth Opening of 15 mm, a Visual Analog Scale pain score of 8 and a dietary score of 4 (International Dysphagia Diet

Standardisation Initiative), presented for consultation and treatment. Virtual surgical planning was used to design a bilateral Xilloc Temporomandibular Joint Prostheses System with custom polyamide surgical (cutting and drilling) guides for bilateral Total Joint Replacement, marking its technology clinical debut in Germany. Temporomandibular Joints Total Reconstructions were executed via combined endoaural and Risdon approaches. Polyamide drilling guides designed with six mandibular ramus pilot drill holes and four zygomatic arch pilot holes, without intermediate splints, were the keystones for preparing the recipient bone. Piezosurgery was used for precise, easier and less traumatic condylectomies guided by the cutting guides. A patient-fitted Ultra-High Molecular Weight Polyethylene articular fossa component was secured to the zygomatic arch using four 2.0-millimeter diameter locking titanium screws. Next, a Three-Dimmensional-printed titanium alloy ramus component, pre-assembled with a Zirconia condylar head, was fixed with six 2.4-millimeter diameter locking titanium screws. A artificial Ultra-High Molecular Weight Polyethylene 9-millimeter disc was bilaterally interposed between condylar head and fossa components to absorb masticatory impact, providing secure and free mandible biomechanical rotational and translational movements. Active physical therapy started on day three, enabling stable functional recovery and an unconstrained return to solid foods diet. At the 72-month follow-up patient presented with zero CMD and/or Temporomaibular Joint pain, stable occlusion and normal dietary pattern.

Results: Postoperative recovery was uneventful without any Cranial Nerve VII branches temporary paralysis, absolute mechanical stability or foreign body tissue reactions. At 12-month follow-up, the patient achieved a stable maximal mouth opening of 36-millimeter, unconstrained dietary efficiency, complete resolution of previous chronic bilateral joint pain, maintaining a well-balanced aesthetic face. Postoperative CT scan confirmed perfect alignment, demonstrating an ideal anatomical bone-implant interface and perfect adaptation. At 72-month landmark evaluation, this comprehensive longitudinal milestone demonstrated exceptional long-term functional stability and optimal biocompatibility of the patient-personalized prosthetic interfaces. The patient reported absolute satisfaction with the customized alloplastic total joint replacement, yielding profound, permanent improvements in objective Patient-Reported Outcome Measures and global Quality of Life.

Conclusion: The custom-manufactured Xilloc Temporomandibular Joint Prosthesis System for Total Joint Reconstruction offers an exceptional anatomical fit and favorable long-term biomechanical performance, drastically cutting surgical time due ultra-precise, additively manufactured and ergonomically optimized patient-spefcific surgical guides, enhancing functional Quality of Life for end-stage Temporomandibular Joint patient after 72-month follow-up.

Keywords: Temporomandibular Joint Prosthesis; TMJ Implant 3D Laser Printing, Xilloc TMJ Prosthesis System; Xilloc TMJ Implant System

Introduction

End-stage disorders of the Temporomandibular Joint (TMJ), such as severe fibrous or bony ankylosis, extensive condylar loss from trauma or neoplasia, advanced degenerative osteoarthritis and multi-operated failed autogenous reconstructions, cause dramatic functional impairments and they impose an every-case challenge in Oral and Maxillofacial Surgery (OMFS). Patients in those conditions always suffer from one or several of these following conditions: a) severe restriction of masticatory function, b) airway obstruction, c) chronic TMJ pain, d) chronic cervifacial myofascial pain and e) progressive dentoskeletal facial deformities, worsening local and general health condition with the time if no treatment is done.

As established by Al-Moraissi, et al.[1], when conservative measures and autogenous grafts fail or are contraindicated due to a high recurrence risk, alloplastic customized or Patient-Specific (Pt-S) TMJ Total Joint Replacement (TJR) stands as the gold-standard therapeutic path.

Historically, stock or prefabricated alloplastic prostheses were utilized. However, as demonstrated by Westermark[2], these stock devices require extensive intraoperative adaptation extending general anesthesia and its risks, manual bone contouring, surgeon's creativity to improvise and frequently deliver suboptimal anatomical devices seating in cases of severe facial asymmetry and/or distorted mandible and temporal bone geometry. To bypass these drawbacks, Dobbe, et al.[3] emphasized how Computer-Aided Design and Computer-Aided Manufacturing (CAD/CAM) along with Three-Dimmensional (3D)-printing technologies have revolutionized Oral and Maxillofacial reconstruction surgery.

The Xilloc Temporomandibular Joint Prosthesis (Xilloc Medical Int. B.V., Sittard-Geleen, Netherlands) represents a peak in this evolutionary timeline. As detailed by Merema, et al.[4], this system is based on the historically validated biomechanical principles of the Groningen total joint prosthesis, merging patient-specific Computed Tomography (CT) data with modern additive manufacturing techniques.

The primary objective of this scientific paper is to comprehensively delineate the engineering, technical parameters and material features of the Xilloc TMJ Prosthesis System (X-TMJ-PS). Furthermore, we illustrate its real-world clinical execution and functional predictability through a detailed surgical description and a long-term clinical outcomes (6-year follow-up) report of the very first patient submitted to TJR with X-TMJ-PS in Germany.

Technical Profile: The Xilloc Patient-Specific Total Joint Prosthesis System

The X-TMJ-PS is a Pt-S, alloplastic joint replacement devices developed in strict collaboration with the University Medical Center Groningen, The Netherlands. It structurally builds upon the clinically validated in the past "Groningen TMJ Prosthesis" concept[4]. From that structural model it turned out to be the most advanced assembly of interconnected components virtually designed to interact as a system, transferring (muscular) bioforces to produce controlled (mandible) biomotion.

This section below breaks down the engineering specifications, mechanical tolerances and industrial manufacturing architecture of the X-TMJ-PS.

Kinematic mechanics and design philosophy

Standard stock TMJ prosthesis function primarily as a constrained or semi-constrained ball-and-socket joint, compressing functional loads into a tight rotation vector[2]. In contrast, X-TMJ-PS separates translation from rotation to closely replicate natural mandibular kinematics, a principle engineered to minimize long-term strain on the cranial base[1,5].

- **Rotational component:** Achieved via true alignment of the custom-milled condylar head within the primary valley of the polyethylene articular fossa[5].
- **Translational component:** Replicated by customized contouring of the artificial articular eminence. During protrusion and lateral excursions, the condylar module glides forward along an engineered slope, preventing mechanical locking and maximizing lateral jaw excursion ranges[4].

Additive manufacturing, materials and surface engineering

Xilloc TMJ implant components are produced using advanced medical-grade manufacturing tracks, tailored to meet or exceed international American Society of Testing Materials (ASTM) and International Standards Organization (ISO) standards for class III medical hardware, which is a high-risk, life-sustaining implantable medical device[6].

Mandibular ramus component (Additive printing track)

- **Material:** Medical-grade Titanium (Ti) alloy (Ti6Al4V ELI - Extra Low Interstitials - Grade 23 / ASTM F136)[6].
- **Manufacturing method:** Selective Laser Melting (SLM) / Direct Metal Laser Sintering (DMLS). High-precision micro-lasers fuse raw Ti alloy dust particle-by-particle in an inert Argon gas chamber based on 3D-virtual design data[3,6].
- **Dual-surface architecture:**
  - **External layer (Functional Surface):** Finished to a completely solid, satin-polished texture to reduce soft-tissue friction, avoid muscle attachment and ensure structural rigidity[6].
  - **Internal layer (Bone-Facing Interface):** Engineered as an unpolished, highly structured porous 3D-Ti lattice mesh[6]. As demonstrated by Gruber and Taschner (6), the pore sizes range precisely between 300 to 500 µm, with an open porosity of approximately 60–70%. This specific micro-architecture mimics human trabecular bone geometry, maximizing immediate mechanical friction and triggering rapid endosseous ingrowth (osseointegration) without requiring extra bone-cement.

Condylar head module (Tribological Core)

- **Material options:** Medical-grade Zirconia (ZrO_2) ceramic or surgical-grade Cobalt-Chromium-Molybdenum alloy (Co-Cr-Mo / ASTM F75)[5].
- **Surface geometry:** The structural sphere is polished using automated diamond-lapping machinery to a mirror-like finish with an average surface roughness average (Ra) of < 0.02 µm.
- **Tribological rationale:** Zhou and Yang[5] demonstrated that articulating ultra-smooth ZrO2 against Ultra-High Molecular Weight Polyethylene (UHMWPE) lowers the friction coefficient by up to 40% when compared to traditional Ti-on-UHMWPE stock combinations. This configuration significantly reduces material wear debris, preventing the local macrophage activation that causes late aseptic loosening and osteolysis[5,7].

Articular fossa component - Cranial plate

- **Material:** Medical-grade solid UHMWPE machined via high-speed 5-axis Computer Numerical Control (CNC) milling from consolidated stock blocks[5].
- **Adaptation mechanics:** The superior surface of the UHMWPE plate copies the exact geometric contours of the patient's native zygomatic arch and glenoid fossa bone as mapped by thin-slice CT scans[1,4]. This structural precision spreads stress loads across the skull base and keeps local pressure concentrations to a minimum[8].

InterFix fixation engineering and pre-calculated vectors

Primary mechanical stability relies on advanced unicortical and bicortical osteosynthesis, minimizing overall peak stress distribution throughout the native bone structure (Figure 1, Force Distribution).

The layout is optimized before the operation using Finite Element Analysis (FEA) software[6].

- **Integrated locking technology:** The screw hole geometries inside the custom Ti plate match the angle of the companion locking screws. Once driven into place, the screw head locks directly into the internal thread of the plate, turning the plate and screws into a unified monobloc system (**Figure 1**, Mandibular Component Integration)[3].
- **Calculated force allocation:** Screw lengths, diameters which are typically 2.0-mm for temporal bone and 2.4-mm for mandibular fixations and paths are strategically aimed away from inferior dental roots and the Inferior Alveolar Nerve canal. Placing screws across multiple distinct vector groups counteracts tensile and torsional stress from masseter and medial pterygoid muscles during normal occlusion and lateral movements (**Figure 1**, Central Stress Map)[9].
- **Recessed profile:** All screw holes feature engineered bevels. As highlighted by Saeed, et al.[9], this configuration ensures that once fully tightened, the screw heads sit completely flush with the metal plate casing, avoiding soft-tissue tension, palpability or localized mucosal breakdown.

Technical schematics and image layout

High-resolution, thin-slice computed tomography data provided the foundational geometric coordinates necessary to design the patient-specific construct components. During VSP phase, engineers pre-calculate the precise anatomical contours, drill trajectories and material thresholds required for each functional module, as summarized in the system architecture matrix **(Table 1)**.

These digital layout parameters are subsequently transferred to automated additive manufacturing tracks to generate custom surgical templates and the interlocking Ti alloplastic prosthesis components with zero geometric tolerance[1,3].

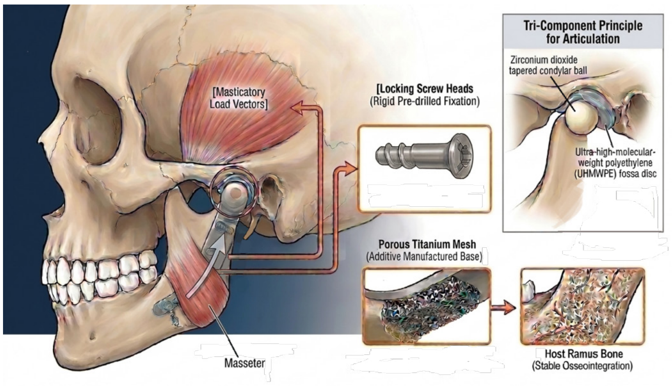

Figure 1: Rationale for biomechanical load distribution and materials architecture of the X-TMJ-PS. The schematic highlights the tri-component articulation system (Zirconia-on-UHMWPE), finite element stress concentration maps within the custom Ti mandibular base and the 3D-printed porous Ti lattice designed to optimize bone ingrowth and long-term stability along the host mandibular ascending ramus.

Table 1: Biomechanical and Material Profile of Pt-S X-TMJ-PS.

Phase / Structural Element	Material Used	Function / Target
Surgical (cutting and drilling) Guides	Polyamide (PA2200) with holes delimited by cylindrical metals	* Bilateral condylectomy and drilling direction templates.
Articular Fossa	UHMWPE	* Replaces natural articular fossa and articular eminence anatomy.
Mandibular Ramus	3D-printed Ti6Al4V	* Customized load-bearing plate adapted precisely to mandibular anatomy.
Condyle	ZrO_2	* Achieves a remarkably low surface roughness.
Disc	UHMWPE with internal Ti markers	* Replaces anatomic fibrocartilaginous disc and it is interposed between fossa and condyle. The internal Ti helps on postoperative CT scan controls.

Notes: Structural and material configuration matrix of the custom-manufactured X-TMJ-PS. The tabular layout catalogs the biomaterial specifications and targeted clinical parameters corresponding to each patient-fitted hardware entity.

Consolidated engineering parameters reference

The critical mechanical, material and geometric requirements dictating the performance of the Pt-S TMJ prosthesis system are consolidated in **(Figure 2)**. The comprehensive matrix cross-references each technical indicator, including the core Ti6Al4V ELI base alloy structural properties, specialized Zirconia-on-UHMWPE articulation boundaries and the functional 300-500 µm porous lattice network configuration, directly with its clinical significance to guarantee optimal osseointegration, fatigue resistance and overall implant longevity.

Case Report

Patient history and clinical presentation

A 56-year-old A.F. (L.D.) was referred to PM's OMFS clinic in Sankt Wendel, Saarland - Germany, on February 6, 2020, complaining of an inability to properly open her mouth, severe difficulties in chewing solid foods, persistent bilateral Cervicofacial Myofascial Disfunctional (CMD) pain, reporting debilitating and unremitting bilateral TMJ arthralgia, quantified as an 8 on a 10-point Visual Analog Scale (VAS; 0 = no pain, 10 = worst imaginable pain). Extraoral photographs are shown in **(Figures 3A-3G)** and intraoral ones in **(Figures 4A-4F)**.

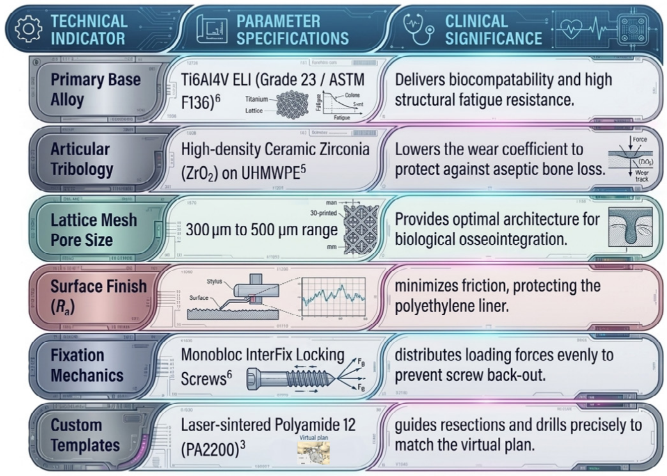

Figure 2: Technical and material specifications of the custom X-TMJ-PS. Summary matrix detailing the biomaterial parameters, manufacturing tracks and clinical rationales for each Pt-S TMJ component.

Patient's medical history revealed autoimmune conditions associated with lupus, taking intermittent short-term steroids to suppress inflammation and calm the immune system attacks, focused to only control severe flare-ups. No previous surgical procedures in the head, face or neck.

Figures 3A-3G: First consultation extraoral photographs of patient's face. (A-B) Frontal view with close mouth and smile (expression of facial discomfort is appreciated). (C-D) Right and left profile views. (E-F) One-third and full caudal-cephalic face view with no facial visible deformities. (G) Patient positioned in Maximum Intercuspation (MI) and aligned by chin, columella and zygomatic bones for correct CT scan exam at the same consultation.

Clinical examination revealed a severe limitation in mandibular range of motion (MROM), with a Maximal Mouth Opening (MMO) of 15 mm. Bilateral lateral excursions were 4-5 mm. The patient's dietary habits were not transitional foods, being restricted entirely from liquids to pureed foods with a dietary scale scoring 4 on the International Dysphagia Diet Standardisation Initiative (IDDSI) (10), as illustrated on **(Figure 3)**.

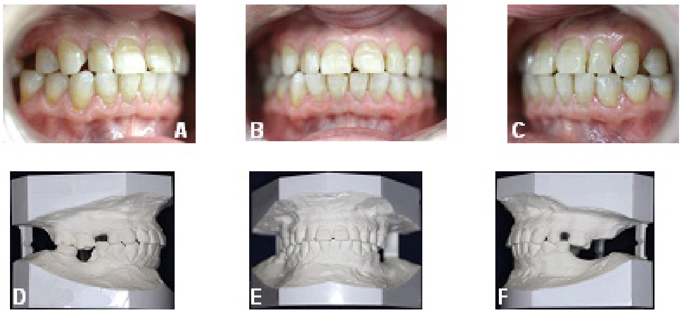

Figures 4A-4F: First consultation intraoral photographs. (A-C) Closed mouth on occlusion on right, center and left views. (D-F) Dental models on occlusion on right, center and left views, mounted for the best and most stable MI. This model occlusion was scanned and shared with Xilloc engineers for X-TMJ-PS construction and final post-operative occlusion. Note a slight discrepancy for the patient's original clinical occlusion and the desired one.

Figure 5: The IDDSI framework consists of a continuum of 8 levels (0 - 7), where drinks are measured from Levels 0 - 4, while foods are measured from Levels 3 - 7. This framework provides a common terminology to describe food textures and drink thickness. © The International Dysphagia Diet Standardisation Initiative 2019 @ https://iddsi.org/standards/framework Licesend under the CreativeCommons Attribution Sharealike 4.0 License https://creativecommons.org/licenses/by-sa/4.0/legalcode.

No muscle or facial nerve paralysis were observed.

TMJ imagings and virtual planning evaluation

Magnetic Resonance Imaging revealed a Wilkes classification (11) stage 4 or Stevão (12) Modified Wilkes Classification as C3I5S5 (C = clinical; I = Imaging; S = Surgical; ranging from 1 to 5), as shown in **(Figures 6A-6B)**.

Three-dimensional volumetric bone reconstruction was obtained from the preoperative CT scan, as depicted in **(Figures 7A-7E)**.

Given the patient's underlying autoimmune condition and the documented poor responsiveness of systemic inflammatory arthropathies to conservative TMJ surgical interventions, a primary TJR was indicated. Consequently, a customized alloplastic TJR utilizing the Pt-S X-TMJ-PS was proposed to bypass the volatile biological environment and deliver predictable, long-term mechanical stability.

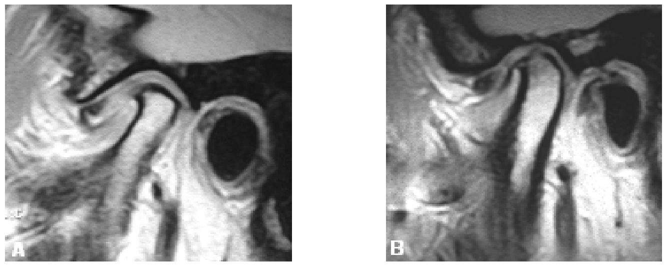

Figures 6A-6B: Magnetic Resonance Imaging (MRI) executed using a high-field 3.0-Tesla scanner, 2-millimeter (mm) slice thickness with 0.2 mm interslice gap, showing severe TMJ structural advanced pathology. (A) Sagittal proton density (PD) and T2-weighted - closed mouth position. Right TMJ was categorized as a high-grade Wilkes Stage IV-V internal derangement. Image demonstrates a severely deformed, structurally fragmented and irreversibly displaced articular disc. Condylar head shows advanced osteoarthritic changes, including flattening, mechanical restrictions, osteophytic flattening of the mandibular condyle and subchondral bone remodeling are identified. (B) Sagittal oblique T1/PD-weighted MRI of the left TMJ - closed-mouth position. Left TMJ graded as Wilkes Stage IV internal derangement. Image depicts permanent anterior disc displacement without reduction. Note the structural deformation of the unsalvageable fibrocartilaginous disc mass located entirely anterior to the condyle, accompanied by advanced osteoarthritic changes including flattening of the condylar head, subchondral sclerosis and osteophytic bone remodeling.

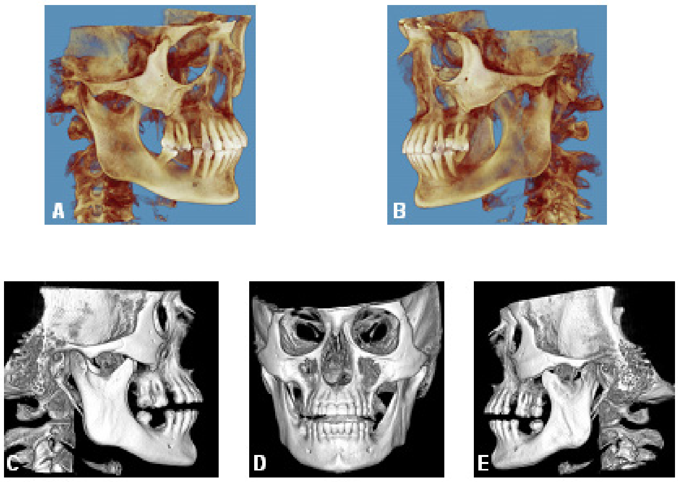

Figures 7A-7E: 3D biomodels virtually reconstructed from CT images. (A-B) Images from the right and left side of the face when patient with closed mouth. (C-E) Images from the right, center and left side of the face when patient is in MMO (15 mm).

Following an exhaustive diagnostic evaluation, a comprehensive counseling session was conducted wherein the patient was fully educated regarding the multi-planar pathology, long-term prognostic vectors and alternative therapeutic modalities.

The patient agreed with the treatment and a complete, signed informed consent was secured after demonstrating absolute comprehension of the planned Pt-S surgical intervention.

A VSP was done by Xilloc head designer at their headquarter. The surgical (cutting and drilling) guides were virtually positioned over the right and left zygomatic root and right and left mandibular ramus to match the exact placement of the screws, as illustrated in **(Figures 8A-8D and 9A-9D)**.

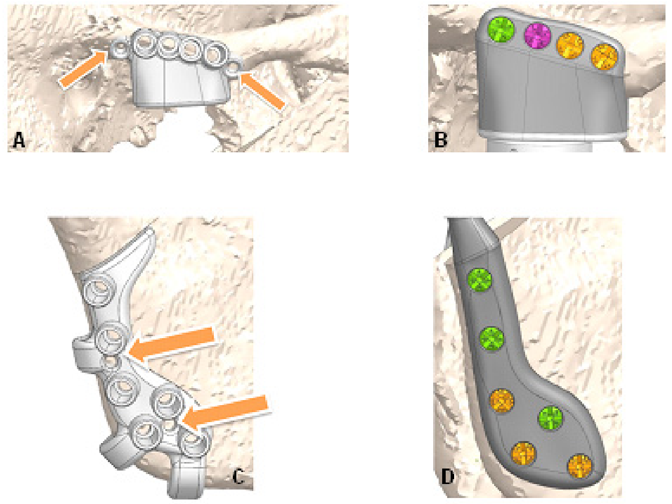

Figures 8A-8D: Description right X-TMJ-PS: Right Fossa Component. (A) Polyamide drilling guide secured in position by 2 x 7-mm non-locking disposable Ti screws, indicated by arrows. (B) Four Ti screws described as 1 x 9-mm green color locking Ti screw, 1 x 7-mm purple color locking Ti screw and 2 x 11-mm locking golden color Ti screws, respectively. Right Mandibular Component. (C) Polyamide drilling and cutting guide secured in position by 2 x 7-mm non-locking disposable Ti screws, indicated by arrows. (D) 3 x 11-mm locking golden color screws and 3 x 9-mm green color locking screws.

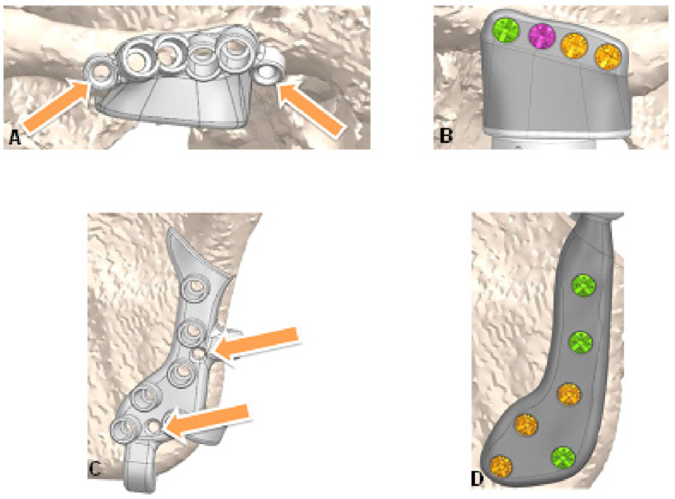

Figures 9A-9D: Description left X-TMJ-PS: Left Fossa Component. (A) Polyamide drilling guide secured in position by 2 x 7-mm non-locking disposable Ti screws, indicated by arrows. (B) Four Ti screws described as 1 x 9-mm green color locking Ti screw, 1 x 7-mm purple color locking Ti screw and 2 x 11-mm locking golden color Ti screws, respectively. Left Mandibular Component. (C) Polyamide drilling and cutting guide secured in position by 2 x 7-mm non-locking disposable Ti screws, indicated by arrows. (D) 3 x 11-mm locking golden color screws and 3 x 9-mm green color locking screws.

Surgical procedure

Patient was operated at the Elisabeth Stiftung Hospital, Elisabeth Foundation of the German Red Cross, located in Birkenfeld, Rhineland-Palatinate - Germany on August 11th, 2020. A whole team was put together for this unique surgical procedure and are seen in **(Figures 10A-10B)**.

Figures 10A-10B: Interdisciplinary team executing the first X-TMJ-PS TJR in Germany. (A) Front row, left to right: Operating room nurses Stephan Quak, Asja and Ludmilla Becker, Mr. Maikel Beerens (Biomedical engineer, Xilloc), Ms. Michaela Schwinn (Surgical assistant) and Prof. Dr. Peter Maurer (Oral and Maxillofacial surgeon). Back row, right to left: Prof. Dr. Eber Luis Steolo (Oral and Maxillofacial surgeon), Mr. Thijs van Leeuwen (Biomedical engineer, Xilloc) and Dr. Pavel Morschanski (Anesthesiologist). (B) Intraoperative placement of the Pt-S implant components under active, on-site technical supervision of Xilloc biomedical engineers to ensure structural alignment, precise seating, anatomical compliance and absolute dimensional accuracy of the X-TMJ-PS.

Under nasotracheal intubation and general anesthesia, an endoaural incision combined with a Risdon (submandibular) approach was utilized to gain access to the left zygomatic arch and mandible. After the TMJ was internally accessed, minescectomy was performed to fully expose the condyle as shown in **(Figure 11)**. All soft tissue in and around the articular fossa were judiciously removed. At this stage, adaptation of the articular fossa drilling guide is deferred due to spatial constraints associated with the minimally invasive endoaural approach. Following the completion of condylectomy, adequate anatomical clearance is achieved, significantly facilitating both the precise positioning of the drilling guide and the subsequent insertion and rigid fixation of the final fossa component.

Figure 11: Intraoperative view demonstrating the complete removal of the left TMJ articular disc and retrodiscal tissue, facilitating enhanced visualization of the osseous structures and expanding the intra-articular space.

Then, a Risdon incision was performed, local tissues dissected followed by periosteal detachment to mandible angle and ascending ramus fully exposition. The lower polyamide surgical guide was inserted and perfectly adapted to the mandibular ramus bone surface by its three flanges and secured in position by two equidistants screws. Procedures observed in **(Figures 12A-12D)**.

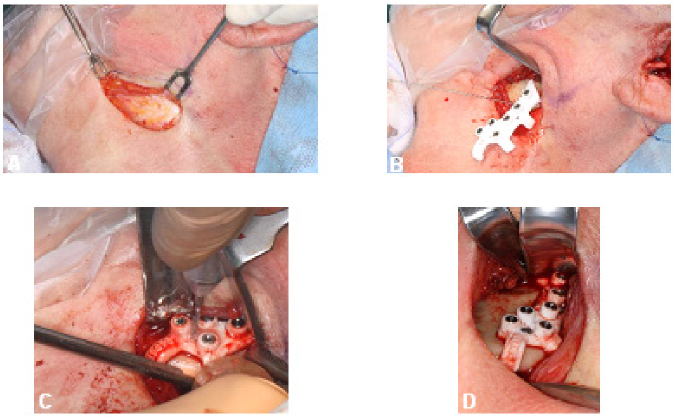

Figures 12 A-12D: Intraoperative view demonstrating the surgical exposure of the mandibular angle and ascending ramus via Risdon approach. (A) The surgical field illustrates sharp anatomical dissection and layer-by-layer soft tissue retraction. (B) This exposure reveals the underlying mandibular osseous surface while preserving the marginal mandibular branch of the facial nerve and adjacent facial vasculature. The patient-specific polymer cutting and drilling guide is inserted and seated in position. Surgical twisted # 1 wire is passed through a small perforation at the mandible angle to facilitate mandible traction. (C) Drilling through polymer and bone for guide fixation with 2-mm dia. Ti non-locking screw. (D) Surgical guide secured in its final position for pre-holes drilling. This caudal surgical portal provides direct visualization and unhindered instrument access required for the precise anatomical placement, adaptation and rigid internal fixation of the custom mandibular guide and final implant shaft.

By applying superior displacement to the mandibular angle toward the articular fossa, a piezo-condylectomy is executed through the endoaural incision and not Risdon approach. This procedure is entirely facilitated by a single, dual-purpose patient-specific surgical template that guides both the pre-drilling and the subsequent osteotomy line, as illustrated in **(Figures 13A-13B)**.

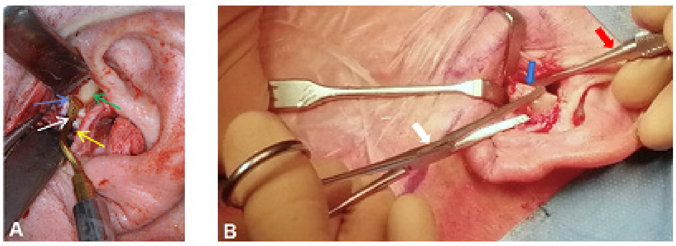

Figures 13A-13B: Intraoperative view of the endoaural surgical approach used for left TMJ arthroplasty utilizing piezosurgery. The clinical fields demonstrate soft tissue retraction exposing deep subfascial plane anterior to the external auditory canal. (A) A specialized long piezoelectric ultrasonic osteotome tip/insert OT12 (white arrow) is engaged at the bony interface determined by the cutting guide (blue arrow), performing a precise, micro-vibrational condylectomy (green arrow). Yellow arrow shows the superior 2.0-mm dia. non-locking disposable Ti screw used for surgical guide fixation. Note the condyle complete stripped out of its periosteum. (B) The left condyle (bold blow arrow) is hold by an Allys clamp (bold white arrow), twisted for easier removal of the small surgical site helped with outward force exerted by Seldin retractor (red bold arrow). Note that the superior aspect of the inverted condyle fragment (blue bold arrow) shows a precise linear osteotomy provided by piezosurgery.

Bilateral coronoidectomies were deliberately omitted, as anteroposterior (AP) mandibular translation was not indicated for the definitive maxillomandibular position. Following the completion of the planned condylectomy and pre-holes on this left side, the Pt-S mandibular surgical guide was carefully unseated and removed from the operative field.

Next step, the upper polyamide drilling guide was locked onto the zygomatic root, fixed in position with two ending screws and subsequently all four holes were carefully drilled. After completion of this step, the drilling guide was removed, as depicted in **(Figures 14A-14C)**.

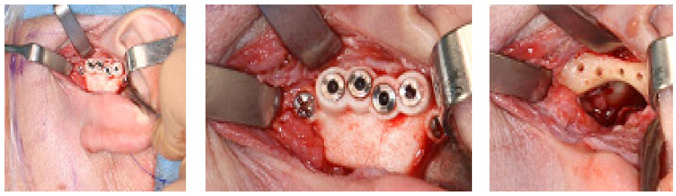

Figures 14A-14C: Intraoperative view of the endoaural approach demonstrating the Xilloc patient-specific TMJ drilling guide fixation. (A-B) The surgical field illustrates the exposure of the zygomatic through anatomical tissue retraction. A custom-machined bone-borne surgical drilling guide is rigidly seated against the native cortical bone profile with two monocortical 2.0-mm dia. disposbale Ti screws. This Pt-S positioning fixture ensures highly predictable and accurate reproduction of the preoperative VSP for subsequent screw-hole pre-drilling. (C) Drilling guide removed showing pre-holes at the left root of the zygomatic process of the temporal bone.

Hemostasis of both left surgical sites was maintained via temporary mechanical packing with saline-moistered gauze pads, for the identical sequence of osteotomy, drillings and component adaptations on the contralateral side.

After maxillomandibular fixation (MMF) was obtained using patient own final occlusion (no intermediate acrylic splint used), the insertion of Xilloc implants started on the right side, adapting first the custom UHMWPE glenoid fossa component which was introduced and secured in position with three Skull Centre Ti Pins oriented by the pre-holes. Rigid internal fixation of the fossa component in its optimal anatomical seat was completed using four 2.0-mm dia. Ti locking screws, with their length pre-determined by VSP, as illustrated in **(Figures 15A-15B)**.

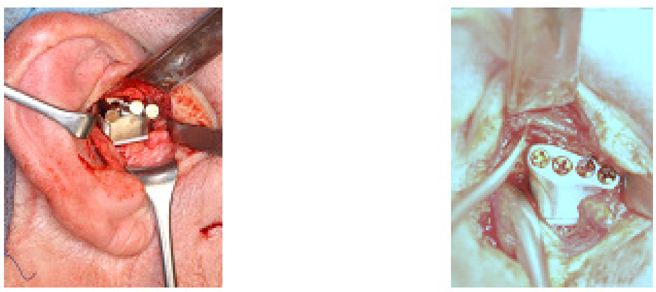

Figures 15A-15B: Intraoperative view demonstrating the left patient-specific surgical template seated directly against the articular eminence and zygomatic arch profile. (A) The custom guide features three Ti cylinders (Skull Centre Ti Pins) designed to ensure precise directional orientation and path-of-insertion alignment for subsequent 2.4-mm dia. Ti screw insertion into pre-drilled holes, confirming strict fidelity to the preoperative VSP.

Subsequently, the 3D-printed Ti mandibular component (shaft), pre-assembled with the Zirconia condylar head, was inserted via submandibular approach and fixed in position after secured by five Mandibular Centre Pins guided by the pre-holes, as well. The mandibular component was fully secured in position with six specific-measure 2.4-mm dia. locking Ti screws, as seen in Figure 16. Definitive stabilization of the mandibular component was achieved using six 2.4-mm dia. Ti locking screws, with length pre-determined on VSP, ensuring adequate rigid internal fixation as demonstrated in **(Figure 16)**. The artificial disc was positioned against the Zirconia condylar head for precise vertical delimitation.

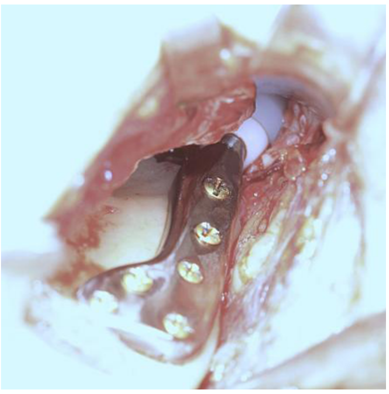

Figure 16: Intraoperative view demonstrating the definitive seating and rigid internal fixation of the left X-TMJ-PS for TJR. Superiorly, the artificial condylar head component is cleanly and fully articulated with the UHMWPE 9-mm disc, successfully reconstructing the joint anatomy and restoring functional structural continuity.

Both implants adapted flawlessly to the bone contour without requiring any manual modification, under constant check of both engineers present in the surgical room as depicted in **(Figure 8B)**.

Identical surgical procedures and fixation protocols were replicated on the left side for both articular fossa and mandibular components. Following the completion of all reconstructive phases, intraoperative occlusion was meticulously checked prior to and following the disassembly of the MMF to confirm optimal occluding stability.

Following an exhaustive inspection of the surgical beds and meticulous microstructural hemostasis revision via bipolar electrocoagulation, anatomical layer-by-layer closure of the four operative sites was systematically executed. For the deep fascial planes, the musculus Temporalis anchorage, the periosteal margins of the zygomatic root and the pterygomasseteric sling, structural adaptation was secured utilizing interrupted resorbable 3-0 and 4-0 polyglactin 910 sutures. The superficial muscular aponeurotic system (SMAS) and subcutaneous tissues were aligned to minimize dead space and eliminate tension across the cutaneous margins. Cutaneous adaptation along the endoaural crease lines and the submandibular Risdon paths was finalized utilizing a continuous non-resorbable 5-0 monofilament nylon suture configured for precise subcuticular skin closure to optimize long-term aesthetic scar remodeling. No capillary drainage system was used.

Postoperative management and 72-month outcomes

The postoperative healing phase proceeded uneventfully. Meticulous clinical monitoring revealed no parameters of localized or systemic infection, nor any structural signs of acute bio-incompatibility or implant rejection throughout the early follow-up period.

Immediate postoperative before nasotraqueal tube extubation, occlusion and checked and neurological evaluation confirmed the complete preservation of all motor branches of the Cranial Nerve VII, with no transient or definitive facial nerve paresis detected during the immediate 12-hour postoperative window, as illustrated in **(Figures 17A-17F)**.

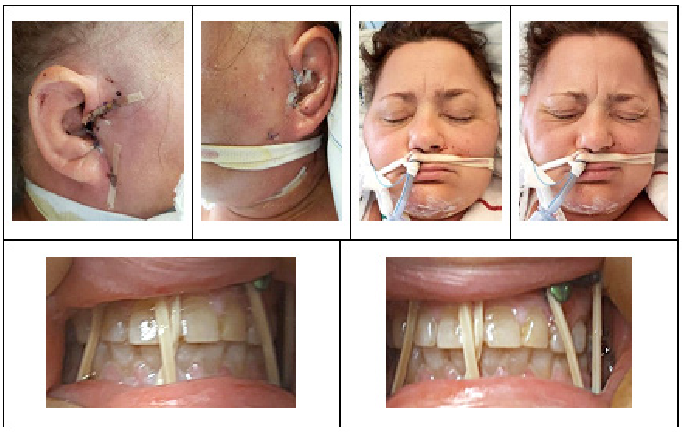

Figures 17A-17F: Early postoperative status of endoaural incisions and postoperative clinical presentation and neuromuscular assessment prior to extubation. (A-B) Endoaural surgical site demonstrates layered cutaneous approximation along the preauricular crease utilizing fine interrupted monofilament sutures, protected by tension-relieving skin strips. Incisions are protected with antibiotic gel. A passive ribbon holds the nasotraqueal tube in position. (C) Patient demonstrates secure airway maintenance via nasotracheal intubation, allowing unobstructed access to the oral and maxillofacial complex during the first hours post surgery. The presence of moderate, expected post-surgical edema is noted, with intact, symmetrical resting facial muscle tone indicating stable preservation of Cranial Nerve VII peripheral branches. (D) Following targeted verbal commands to activate the muscles of facial expression, the patient displays symmetrical forehead corrugation, synchronous brow elevation and balanced bilateral Orbicularis oculi contraction. This coordinated motor function confirms the stable intraoperative preservation of the peripheral motor branches of Cranial Nerve VII, bilaterally. (E-F) Intraoral view showing occlusal alignment and training elastics. The dentition demonstrates stable primary MI and perfect midline alignment matching the VSP targets. Vertical, low-force intermaxillary training elastics are utilized to provide light neuromuscular guidance and maintain occlusal tracking during early rehabilitation, while preventing open-mouth posturing from transient masseter hypotonia.

An immediate postoperative panoramic radiography and CT scan obtained on the first follow-up day post-extubation confirming anatomically precise alignment of the bilateral alloplastic joint components and stable seating of the locking hardware, illustrated across **(Figures 18, 19, 20A-20C and 21A-21B)**.

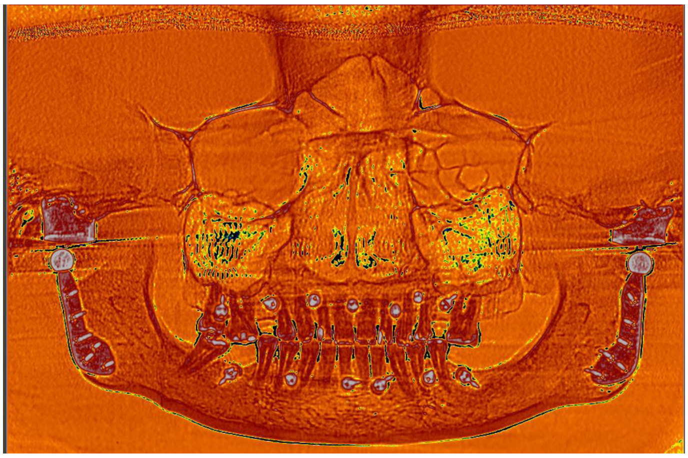

Figure 18: Postoperative panoramic radiographic assessment of the bilateral Pt-S X-TMJ-PS used for TJR. The imaging confirms precise anatomical congruency of the custom-fitted implants along the mandibular borders and zygomatic arches, adequate screw bicortical stabilization and correct vertical ramus height restoration.

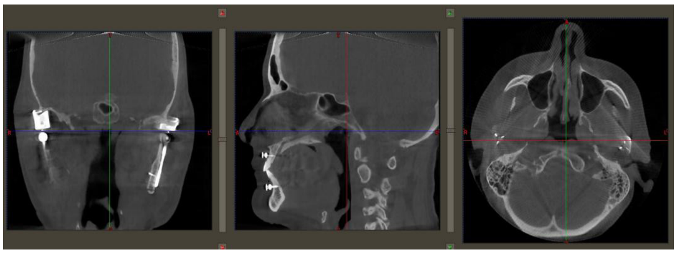

Figures 19A-19C: Postoperative multiplanar CT scan showing 3D anatomical alignment of the patient-specific 3D-printed total TMJ prosthesis system. The reference lines illustrate symmetrical positioning across all anatomical planes: coronal (A), sagittal (B) and axial (C), no signs of devices mechanical dislodgments, demonstrating rigid osteosynthesis fixation and harmonious integration of the artificial condylar heads within the superior articular contours.

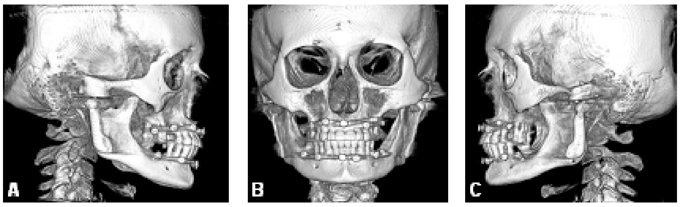

Figures 20A-20C: (A-C) Right lateral, frontal and left lateral of a 3D-CT craniomaxillofacial reconstruction displaying bilateral X-TMJ-PS in situ. The volume-rendered image highlights precise anatomical adaptation of the custom mandibular implants to the native osseous structures, complete restoration of the vertical ramus height and symmetric vertical facial alignment. Concomitant maxillomandibular fixation screws are visible on maxilla and mandible.

Upon hospital discharge, low-tension intermaxillary training elastics were applied for a restricted multi-day period. This non-rigid guidance matrix was utilized to provide neuromuscular proprioceptive feedback and counteract transient musculus Masseteris hypotonia secondary to prolonged intraoperative immobilization, thereby preventing prolonged open-mouth posturing. Guided by these directional elastic vectors, a structured, patient-specific functional maxillofacial physical therapy protocol was successfully initiated on the third postoperative day.

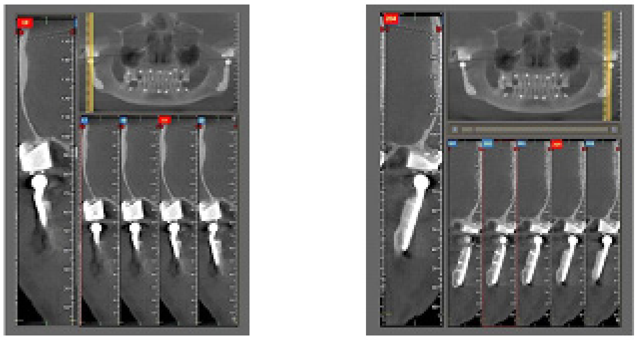

Figures 21A-21B: Postoperative multiplanar CT evaluation of the Pt-S X-TMJ-PS TJR. (A) The panel features a coronal panoramic-like overview (top right) tracking the sectioning planes, alongside a magnified paraxial/cross-sectional view (left, slice 19) and a sequential cross-sectional array (bottom right, slices 17-20). (B) Tracking scout (top right) marking the precise cross-sectional planes, a magnified paraxial view (left, slice 204) and a sequential paraxial cross-sectional array (bottom right, slices 201–205). The two radiopaque points of the articular discs can be appreciated on slices 19 and 204. The CT imaging demonstrates precise, concentric seating of the radiopaque prosthetic condylar head within the superior custom articular component, preserving correct structural orientation and showing no signs of components displacements.

The postoperative phase prioritized early mobilization to exploit the low friction properties of the custom Zirconia-UHMWPE articular track[5]. On postoperative Day 2, the patient initiated a structured four-phase functional rehabilitation protocol illustrated at **(Table 2)**. Early goals focused on passive range expansion and edema management, safely transitioning into aggressive active resistance exercises by Week 7[3]. This chronologically targeted physical therapy track was vital in preventing regional muscle atrophy and soft-tissue guarding, allowing the patient to safely transition from a strict liquid diet to unconstrained solid food mastication by the 12-month follow-up[9,13].

At 72-month follow-up evaluation, patient displayed an outstanding increase in jaw mobility, with an MMO of 36 mm, representing an absolute improvement of 21 mm from the initial 15 mm.

Lateral excursive movements were marked at 6-7 mm bilaterally, reduction which was expected due to Musculi pterygoideus lateralis complete detachment during condylectomies but slightly compensated by Musculi temporalis.

Patient reported a complete absence of chronic arthralgia with a VAS dropping from score 8 pre-operatively to score 0 (zero) post-operatively.

Her dietary profile successfully shifted to a normal, unrestricted solid diet (IDDSI score 7), with detailed specifications outlined in previously presented **(Figure 3)**.

Longitudinal tracking of our patient's recovery metrics is presented in the 3D clinical outcomes matrix in **(Figure 22)**. The graphical data contrasts the pre-operative status with the 72-month post-operative outcomes across three key physiological parameters. Following the bilateral alloplastic reconstruction, the baseline chronic arthralgia score decreased from a VAS rating of 8 to a post-operative score of 0. Simultaneously, the MMO increased from an initial 15 mm to a post-operative measurement of 36 mm. Accompanying these functional changes, the patient's nutritional status transitioned from a restricted liquid/pureed dietary regimen to an unrestricted International Dysphagia Diet Standardisation Initiative (IDDSI) level 7 solid diet.

Table 2: Postoperative Physical Therapy and Functional Rehabilitation Protocol Following X-TMJ-PS Replacement.

Phase / Timeline	**Rehabilitation Objectives & Therapeutic Focus**	**Specific Exercises & Clinical Modalities**	**Dietary Progression Matrix**	**Target Benchmarks**
Phase I	* Control immediate postoperative edema.	* Gentle passive jaw opening using a wooden spatula stack.	Strict liquid diet only	* Maximal Mouth Opening (MMO) ≥ 15 mm.
(Days 2–7)	* Prevent early joint capsule stiffness.	* Mild active-assisted opening within non-pain ranges.	(Non-masticatory caloric intake)	* Controlled localized pain scales.
	* Protect primary surgical incision sites.	* Isometric temporalis and masseter contractions.		* Zero tracking deviation on opening.
	* Maintain facial nerve mobility loops.	* Dynamic facial expression exercises (forehead wrinkling, smiling).		
Phase II	* Transition from passive to active mobilization.	* Active jaw opening exercises using a calibrated mechanical thumb-screw device.	Pureed / Soft-processed diet	* MMO reached ≥ 25 mm.
(Weeks 2–6)	* Re-establish bilateral condylar translation tracking.	* Manual soft-tissue stretching of *musculi Masseteris* bellies.	(Blenderized meals, no solid shearing)	* Lateral excursion range ≥ 2 mm.
	* Prevent muscle guarding and spasm loops[3].	* Gentle bilateral lateral excursive translation movements.		* Complete primary scar healing.
		* Contralateral jaw translation stretches.		
Phase III	* Rebuild masticatory muscle strength.	* Progressive resistance jaw opening using custom elastic bands.	Soft solid diet	* MMO reached ≥ 32 mm.
(Weeks 7–12)	* Optimize long-term joint kinematics.	* Advanced lateral excursions against manual finger resistance.	(Masse, cooked vegetables, fish, soft meats)	* Lateral excursion range ≥ 3 mm.
	* Eliminate residual scar tissue boundaries[3].	* Concentric/eccentric open-close control cycles.		* Symmetrical jaw tracking paths.
		* Deep transverse friction massage over healed incision lines.		
Phase IV	* Consolidate complete functional range.	* High-repetition maintenance active MROM stretches.	Normal solid diet	* Stable MMO ≥ 35–36 mm.
(Months 4–12)	* Achieve long-term joint stabilization[9].	* Advanced neuromuscular coordination chewing exercises.	(Unrestricted solid food mastication)	* Unconstrained mastication profiles.
	* Return to unconstrained daily living indexes.	* Targeted long-term stretching protocols executed twice daily.		* Pain-free translation index (0/10).
		• Final functional range verification checkpoints.		

Notes: Visual schematic workflow describing the postoperative protocol. The diagram summarizes the consecutive chronological phases, technical targets and author reference links[3,5,9] specifically built into the custom X-TMJ-Pt-S rehabilitation path.

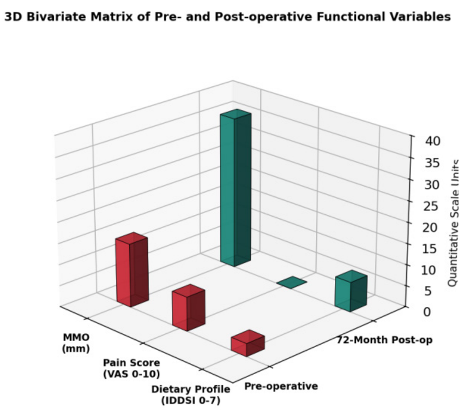

Figure 22: Three-D bivariate matrix tracking long-term structural and symptomatic changes. The pre-operative cohort row (crimson) highlights the initial MMO 15 mm, debilitating arthralgia (VAS 8) and mechanical dietary restrictions (IDDSI Level 3). The 72-month post-operative row (green) details the definitive physiological resolution following bilateral alloplastic TJR with Xilloc custom 3D-printed Ti prothesis system.

At 72-month long follow-up, clinical examination confirmed a harmonious face and stable occlusion, shown in **(Figures 23A-23H)**.

Also, new CT scan was obtained confirming the excellent stable position of the bilateral Xilloc TMJ prosthesis, bone healed, no residual facial and neck soft tissue edema as observed in **(Figures 24A-24F)**.

Discussion

The surgical management of end-stage, advanced degenerative TMJ osteoarthritis (osteoarthrosis) represents a complex reconstructive dilemma in OMFS. As noted by Al-Moraissi et al. (1), when progressive cartilage destruction, subchondral bone remodeling, osteophyte formation and severe joint space narrowing fail to respond to conservative treatments, joint mobility becomes profoundly compromised. While autogenous options such as costochondral grafts are sometimes considered.

Mercuri[14] argued extensively that autogenous tissue remains highly unpredictable in adult populations due to the risk of donor-site morbidity, erratic calcification and unpredictable functional resorption when placed into an actively arthritic, biochemically hostile joint environment. Consequently, alloplastic TJR has become the gold-standard pathway, effectively preventing progressive occlusal instability and enabling immediate postoperative physical therapy.

Figure 23A-23H: Comprehensive 6-year postoperative clinical and intraoral evaluation. (A-E) Extraoral photographs demonstrating harmonic facial aesthetics, balanced facial symmetry at rest and during smiling, normal submental contours and stable lateral profile projections. (F-H) Intraoral views confirming stable dental occlusion, proper intercuspation without midline deviation.

Because the patient's autoimmune profile significantly increases the risk of recurrent fibro-osseous remodeling and mechanical failure following traditional joint-preserving procedures, conservative surgical modalities were contraindicated. To mitigate the hyper-inflammatory response inherent to systemic autoimmune arthropathies, a definitive TJR via a CAD/CAM Pt-S X-TMJ-PS was recommended as the optimal path to ensure structural predictability. This clinical strategy directly aligns with the broader consensus established in modern Oral and Maxillofacial literature; as argued extensively by Mercuri[8,15] and supported by regional data from Stevão[13], custom alloplastic interfaces are uniquely capable of isolating the mechanical hardware function from the hostile, volatile biochemical environment of active systemic arthropathies. By introducing an inert, personalized Ti-ceramic barrier, it is possible to effectively bypass the biological cycle of progressive osteophytic destruction that routinely compromises autogenous or standard stock configurations in this complex patient demographic[3,9].

While conventional stock joint systems provide acceptable clinical solutions for standard anatomy, they present clear spatial and mechanical bottlenecks in patients with highly distorted osseous morphology. Stock components require the surgeon to aggressively grind down healthy host bone or manually bend plates to eliminate empty gaps under the hardware. As highlighted by Saeed, et al.[9] in national outcomes data, this manual customization can cause stress concentrations, micro-motions and ultimate hardware failure.

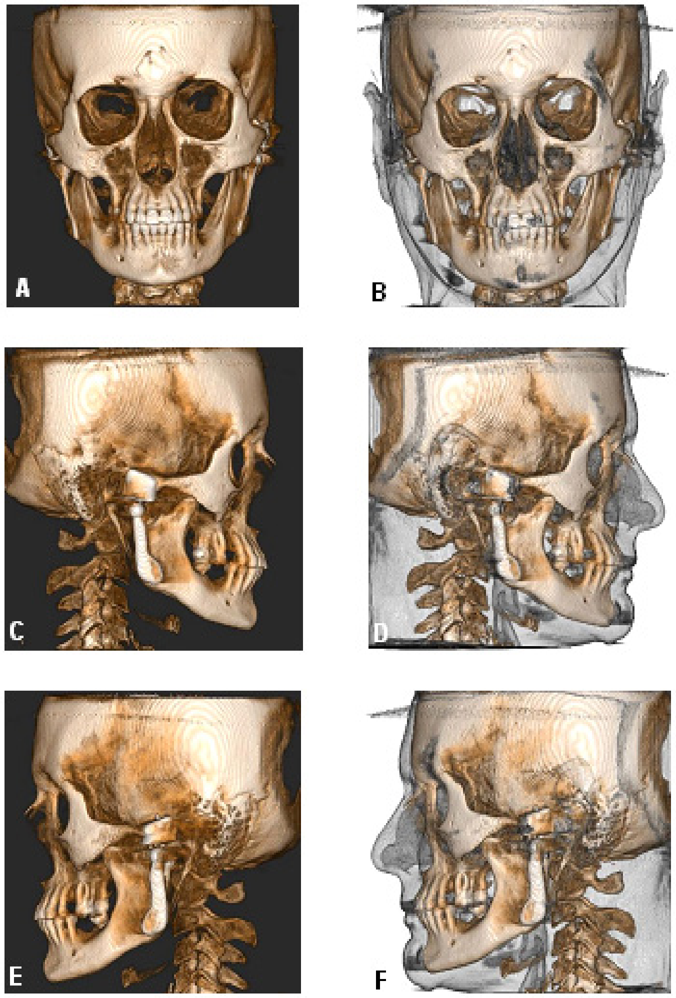

Figures 24A-24F: Postoperative 3D volume--dual-rendered CT reconstructions (hard-tissue versus semi-transparent soft-tissue views), demonstrating precise bilateral X-TMJ-PS positioning, rigid multi-screw fixation and excellent contour adaptation relative to both the osseous architecture and the overlying soft-tissue facial profile. (A,C,E) Highlighting the frontal, right lateral and left latereal skeletal structures alone. (B,D,F) Superimposed frontal right lateral and left lateral with soft-tissue transparent overlays confirms anatomical harmony between the custom-engineered hardware and the overlying facial soft-tissue drape.

To resolve these anatomical discrepancies, Stevão[13] emphasized that Pt-S customized total alloplastic joint systems provide superior biomechanical predictability over standard stock options in complex skull geometries. By bypassing the physical strain of manual intraoperative plate bending, custom systems maintain structural integrity and reduce internal material fatigue, which significantly minimizes the incidence of late device failures.

In contrast, the custom XTMJS provides a completely adapted, pre-planned anatomy. By starting from the patient's individual 3D-CT data, the titanium ramus plate is additively manufactured via SLM to conform exactly to the native bony valleys and ridges, a benefit championed by Merema, et al.[4]. This intimate bone-to-metal adaptation maximizes primary stability and distributes mechanical functional loads more evenly.

The author waited for a long follow-up of 72 months to securely report the case underscoring multiple clear clinical and operatory benefits of this technology:

- **Reduction in operative time:** Because the osteotomy lines, screw channels and plate adaptations are fully predetermined and executed using custom polyamide templates, intraoperative guesswork is eliminated. Dobbe, et al.[3] showed that this predictability significantly shortens the total anesthesia duration and lowers the risk of surgical site infections.
- **Biomechanical harmony and wear reduction:** The tribological combination of a Zirconia condylar head articulating with a high-density UHMWPE fossa plate mimics natural joint friction dynamic. Zhou and Yang[5] observed that the smooth surface of Zirconia drastically slows down UHMWPE wear compared to classic rough metals, minimizing the risk of aseptic loosening induced by particle debris.
- **Engineered osseointegration:** The selective application of a porous lattice design on the inner surface of the 3D-printed titanium component triggers excellent osteoconduction. Gruber and Taschner[6] showed that host bone cells migrate directly into these custom-printed porous gaps, transitioning the implant from simple screw retention to true biological integration.

The 72-month clinical and functional outcomes observed in our patient underscore the long-term efficacy and biostability of X-TMJ-PS for TJR. Achieving a maximum mouth opening (MMO) of 36 mm represents a profound restoration of mandibular kinematics, moving the patient from a state of severe, debilitating trismus (15 mm) to a functional range that exceeds the recognized international success threshold of 30 mm for alloplastic TMJ reconstruction[8]. This absolute gain of 21 mm significantly correlates with the precision of virtual surgical planning (VSP) and the utilization of custom-printed Ti components, which precisely replicate the patient's unique anatomical center of rotation.

The post-operative restriction in lateral excursive movements (6-7 mm bilaterally) warrants careful biomechanical consideration. During aggressive mandibular resections or extensive condylectomies necessitated by progressive pathologies like severe osteomyelitis, complete detachment of the musculi Pterygoideus lateralis from the pterygoid fovea is an unavoidable surgical sequela[16]. Because the lateral pterygoid is the primary initiator of mandibular protrusion and contralateral excursion, its loss typically diminishes lateral translational movement. However, the preservation and vector-driven adaptation of the musculi Temporalis and Masseteris sling provided sufficient secondary stabilization to slightly compensate for this deficit, facilitating a balanced, albeit constrained, excursive envelope that did not impede functional speech or mastication.

Long-term studies compiled by Saeed, et al.[9] on Pt-S alloplastic total joint systems demonstrate exceptional durability and high structural integrity. The 72-month longitudinal follow-up of this German premier case mirrors these global patterns, yielding permanent improvements in objective Patient-Reported Outcome Measures (PROMs). The absolute regression of debilitating arthralgia combined with expansion of vertical MROM to a functional baseline of 36 mm, successfully shifts her subjective indices into objective long-term therapeutic success.

From a QoL and dietary perspective, the transition from an exclusively texture-modified liquid/pureed regimen to an unrestricted solid diet (IDDSI Level 7) is highly significant. Protracted reliance on liquidized diets is frequently associated with progressive nutritional depletion, involuntary weight loss and reduced patient satisfaction (17). The mechanical rigidity and structural stability afforded by the custom titanium mandibular corpus framework successfully redistributed masticatory forces across the remaining craniofacial skeleton. This structural reconstitution directly facilitated the rapid downgrading of dietary restrictions. Financially, minimizing the need for specialized dietetic products or long-term enteric support represents a highly cost-effective outcome in geriatric patient care management.

Long-term studies compiled by Saeed, et al.[9] on patient-fitted total joint alloplastic systems show high structural durability and significant improvements in QoL, pain relief and functional dietary scores. The short-term follow-up of our patient mirrors these positive trends, showing an exceptional restoration of MMO from 8 mm to 36 mm and complete relief from chronic pain.

Crucially, the complete resolution of the patient's long-standing, chronic arthralgia, demonstrated by the dramatic decrease in the VAS score from a severe 8 out of 10 pre-operatively to a stable 0 out of 10 at 6 years, validates the choice of an alloplastic articulating surface over autogenous bone grafting. By using a polished metal condylar head articulating against a custom-fit, high-density polymer and/or UHMWPE fossa liner, the procedure eliminates the biological risks of graft resorption, heterotopic bone formation and donor-site morbidity[18]. This long-term pain eradication confirms that custom alloplastic TJR provides predictable, stable and durable symptomatic relief for complex, end-stage craniomaxillofacial defects.

However, custom CAD/CAM prostheses also present certain limitations. As noted by Mercuri[15], these include their higher cost compared to off-the-shelf devices and the typical manufacturing window required for design and printing, which renders them unsuitable for acute trauma or emergency procedures.

Despite these constraints, for complex secondary reconstructions and end-stage for TMJ diseases, the patient-specific X-TMJ-PS represents an invaluable advancement in personalized OMFS.

Conclusion

The patient-specific Xilloc Total Mandibular Joint Prosthesis System is a reliable and highly predictable medical implantable device for reconstructing complex, end-stage TMJ pathologies. Its custom 3D-printed titanium design, combined with an ultra-low-friction Zirconia-UHMWPE interface, provides an exceptional anatomical fit and stable biomechanical fixation after 72 months as presented on this long-term result study.

Xilloc patient-specific virtual workflow dramatically reduces operating time due to the surgical (cutting and drilling) guides, increases anatomical precision placement, lowers the risk of structural failure and significantly enhances long-term jaw function and QoL.

Declarations

- **Ethical considerations:** This study was conducted in accordance with the Declaration of Helsinki for medical private practice. The patient shown herewithin provided a written informed consent for this publication case report and any accompanying clinical images.
- **Artificial intelligence use statement:** An AI language model was utilized strictly for grammatical correction, formatting optimization and structural alignment according to the journal's guidelines.

- **Acknowledgments:** I acknowledge the technical biomedical engineering team at Xilloc Medical B.V., especially Mr. Maikel Beerens and Mr. Thijs van Leeuwen, for their assistance with virtual surgical planning data and implants production. The author wants to express his immense gratitude to Dr. Peter Maurer for making this case possible to be executed in Germany. Also, the author extend his most sincere gratitude to the dedicated interdisciplinary team at the DRK Elisabeth-Krankenhaus (Birkenfeld, Rhineland-Palatinate - Germany) for their pivotal role in the successful execution of first Xilloc TMJ Total Joint Prosthesis Reconstruction done in Germany. Special recognition is due to the specialized operating room nursing staff, specifically Mr. Stephan Quak, Ms. Ludmilla Becker and Ms. Asja, whose technical expertise and perioperative support were fundamental to this pioneering procedure. We also thank the Department of Anesthesiology, particularly Dr. Pavel Morschanski, for their meticulous care and clinical precision throughout the complex intervention. Finally, the author expresses his appreciation to the Hospital Director, Ms. Michaela Lindemann and the administrative leadership team for providing the advanced institutional framework and resources necessary to implement this high-standard, Pt-S surgical solution.

- **Conflict of interest:** The author declares that he has no competing financial or personal interests related to the manufacture or marketing of the prosthetic system described in this paper.

- **Funding:** This research received no specific grant from any funding agency in the public, commercial or not-for-profit sectors.

- **Data availability statement:** The clinical records, imaging files and planning data are stored within the hospital's secure database and can be made available by the corresponding author upon reasonable request.

Abbreviations

Abbreviation	Definition
OMFS	Oral and Maxillofacial Surgery
TMJ	Temporomandibular Joint
Pt-S	Patient-Specific
TJR	Total Joint Replacement
CAD/CAM	Computer-Aided Design and Computer-Aided Manufacturing
3D	Three-Dimensional
CT	Computed Tomography
X-TMJ-PS	Xilloc TMJ Prosthesis System
Ti	Titanium
SLM	Selective Laser Melting
DMLS	Direct Metal Laser Sintering
ZrO_2	Zirconium Dioxide - Ceramic
Co-Cr-Mo	Cobalt-Chromium-Molybdenum
ASTM	American Society for Testing and Materials
ISO	International Standards Organization
Ti-Al-V ELI	Titanium-Aluminum-Vanadium Extra Low Interstitials
Ra	Roughness average
UHMWPE	Ultra-High-Molecular-Weight Polyethylene
CNC	Computer Numerical Control
FEA	Finite Element Analysis
IM	Maximum Intercuspation
MMO	Maximal Mouth Opening
VAS	Visual Analog Scale
IDDSI	International Dysphagia Diet Standardisation Initiative
MRI	Magenetic Resonance Imaging
VSP	Virtual Surgical Planning
MMF	Maxillomandibular Fixation
dia.	Diammeter
mm	Millimeter
PD	Proton Density
AP	Anterior-posterior
QoL	Quality of Life
PROM	**Patient-Reported Outcome Measure**MROM
MROM	Mandible Range of Motion

References

1. Al-Moraissi EA, Wolford LM, Ellis E 3rd, et al. The hierarchy of different treatments for arthrogenous temporomandibular disorders: A network meta-analysis of randomized clinical trials. J Craniomaxillofac Surg 2020;48(1):12-23.
2. Westermark A. Total temporomandibular joint replacement with a stock prosthesis: long-term outcomes. J Oral Maxillofac Surg 2010;68(11):2735-2741.
3. Dobbe JGG, Peymani A, Roos HAL, et al. Patient-specific plate for navigation and fixation of the distal radius: a case series. Int J Comput Assist Radiol Surg 2021;16(3):515-524.
4. Merema BJ, Kraeima J, Witjes MJH, et al. Accuracy of fit analysis of the patient-specific Groningen temporomandibular joint prosthesis. Int J Oral Maxillofac Surg 2021;50(4):538-545.
5. Zhou H, Yang C. Progress of temporomandibular joint prosthesis: a comprehensive review of designs, materials and clinical outcomes. Chin J Stomatol Res 2020;14(1):44-51.
6. Gruber RM, Taschner M. Biomechanical aspects and material characteristics of custom 3D printed Ti6Al4V implants in craniomaxillofacial reconstruction. J Mater Sci Mater Med 2022;33(2):18-29.
7. Ingham E, Fisher J. The role of macrophages in osteolysis of total joint replacement. Biomaterials 2000;21(1):1-13.
8. Mercuri LG. Alloplastic Temporomandibular Joint Replacement: Rationale and Outcomes. Journal of Oral and Maxillofacial Surgery 2012;70(11):2545-2557.
9. Saeed NR, McLeod NM, Hensher R. Temporomandibular joint replacement in the UK: national outcomes data. Br J Oral Maxillofac Surg. 2018;56(6):527-532.
10. IDDSI 2026.
11. Wilkes CH. Internal derangements of the temporomandibular joint. Pathological variations. Arch Otolaryngol Head Neck Surg 1989;115(4):469-477.

12. Stevão ELL. Cirurgia da ATM: Novos conceitos, Anatomia cirúrgica e Técnicas operatórias. 1ª ed. [S.l.]: Gráfica e Editora Art 41; 2014.

13. Stevão ELL. Sistema TMJ Concepts: Próteses personalizadas e de estoque para reconstrução total da articulação temporomandibular (TMJ Concepts System: Custom-made and off-the-shelf prostheses for temporomandibular joint reconstruction). Full Dent Sci 2013;5(17):88-102.

14. Mercuri LG. Total joint reconstruction - autologous or alloplastic. J Oral Maxillofac Surg 2006;64(3):399-403.

15. Mercuri LG. Alloplastic temporomandibular joint replacement: rationale for the Use of custom devices. Int J Oral Maxillofac Surg 2012;41(9):1035-1042.

16. Wolford LM, Rodrigues DB. Joint replacement with patient-matched total joint prostheses. Atlas of the Oral and Maxillofacial Surgery Clin North Am 2015;23(1):59-71.

17. Cataife G, Mansor MM, et al. Economic and nutritional burden of texture-modified diets in dysphagic populations. Clinical Nutrition ESPEN 2021;42,212-218.

18. Gruber S, Martinez-Castillo G, et al. Long-term stability of 3D-printed titanium implants in mandibular reconstruction: A systematic review. International Journal of Oral and Maxillofac Surg 2023;52(4),411-423.